

Conversion of Nitric Oxide into Nitrous Oxide as Triggered by the Polarization of Coordinated NO by Hydrogen Bonding

Chuan-Hung Chuang, Wen-Feng Liaw,* and Chen-Hsiung Hung*

Abstract: Reduction of the $\{\text{Co}(\text{NO})\}^8$ cobalt-nitrosyl N-confused porphyrin (NCP) $[\text{Co}(\text{CTPPMe})(\text{NO})]$ (**1**) produced electron-rich $\{\text{Co}(\text{NO})\}^9$ $[\text{Co}(\text{CTPPMe})(\text{NO})][\text{Co}(\text{Cp}^*)_2]$ (**2**), which was necessary for NO-to- N_2O conversion. Complex **2** was NO-reduction-silent in neat THF, but was partially activated to a hydrogen-bonded species **2**...MeOH in THF/MeOH (1:1, v/v). This species coupling with **2** transformed NO into N_2O , which was fragmented from an $[\text{N}_2\text{O}_2]$ -bridging intermediate. An intense IR peak at 1622 cm^{-1} was ascribed to $\nu(\text{NO})$ in an $[\text{N}_2\text{O}_2]$ -containing intermediate. Time-course ESI(−) mass spectra supported the presence of the dimeric $[\text{Co}(\text{NCP})]_2(\text{N}_2\text{O}_2)$ intermediate. Five complete NO-to- N_2O conversion cycles were possible without significant decay in the amount of N_2O produced.

Reduction of nitric oxide (NO) to nitrous oxide (N_2O) is catalyzed by a nitric oxide reductase (NOR), which has a non-heme/heme binuclear active site at its catalytic center.^[1] However, the details of the catalytic process, including the active species involved in NO coupling, the short-lived adducts of two NO units, and N–O bond cleavage upon N_2O release, are not well-understood. Biomimetic models of non-heme/heme hybridized active centers have been generated to investigate the chemistry of NO reduction;^[2,3] however, only the initial NO coordination at the active site and the ultimate N_2O release were characterized in these functional model studies. The formation of N_2O by the protonation of putative hyponitrite ($\text{N}_2\text{O}_2^{2-}$)-coordinating intermediates has also been studied extensively with a handful of homo-bimetallic and mononuclear complexes.^[4] The diferric hyponitrite porphyrin complex $[(\text{OEP})\text{Fe}]_2(\mu_2, \eta^1, \eta^1-\text{N}_2\text{O}_2)$ was obtained from the reaction of *trans*- $\text{H}_2\text{N}_2\text{O}_2$ and $[\text{Fe}(\text{OEP})]_2(\mu\text{-O})$.^[4c] However, the same diferric μ -hyponitrite complex has never been produced by a radical-coupling reaction of two mononuclear $\{\text{Fe}(\text{NO})\}^7$ $[(\text{OEP})\text{Fe}(\text{NO})]$ units, in which $\{\text{Fe}(\text{NO})\}^7$ is the Enemark–Feltham notation.^[5] These results indicate that a radical-type coupling reaction to give a $\mu\text{-N}_2\text{O}_2$ bridging diferric porphyrin is thermodynamically

unfavorable and kinetically forbidden;^[5] however, a radical-coupling scenario in native NOR can not be ruled out. One critical feature is that the NOR active site forms asymmetric iron-nitrosyl electronic structures, which are not possible in model studies with a single metal complex. Furthermore, the distal water and amino side chains in native NOR may also generate the proton(s) required for NO-to- N_2O reduction to release either OH^- or H_2O .

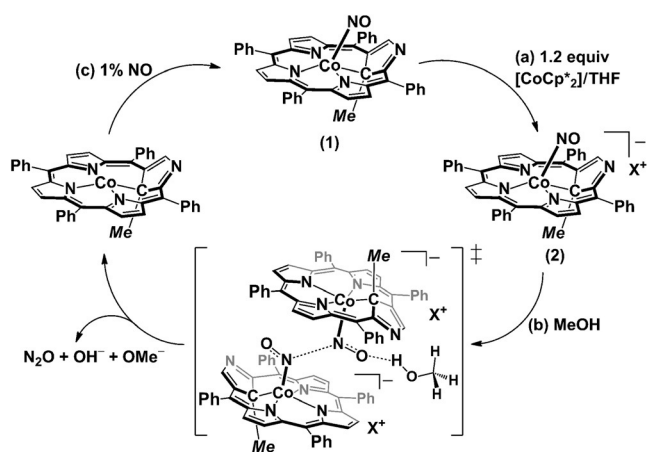
DFT calculations on NO-reduction reactivity with the heme-copper oxidoreductase have indicated that protonation of the heme-nitrosyl group after the initial binding of NO to each of the heme and copper centers results in concomitant N–N bond formation to yield the *trans*-hyponitrite intermediate.^[6] On the other hand, it has been recognized that hydrogen-bonding (H-bonding) interactions ($\text{NO}\cdots\text{HOR}$, $\text{R}=\text{H}$, Me, or Et) that induce electron back-donation from the Cu center to the $2\pi^*$ orbital of NO to facilitate N–O bond cleavage play a crucial role in catalytic NO reduction.^[7] Accordingly, protonation or electrostatic H-bonding interactions exerting force on the O_{NO} atom of the heme-NO moiety could be a crucial driving force for N–N coupling and N–O cleavage reactions. Nevertheless, the addition of a proton source to $\{\text{Fe}(\text{NO})\}^8$ iron-nitrosyl porphyrins leads to the exclusive release of H_2 and a return to the corresponding $\{\text{Fe}(\text{NO})\}^7$ complex.^[8] Although $\{\text{Fe}(\text{HNO})\}^8$ $[\text{Fe}(\text{3,5-Me-BAPP})(\text{HNO})]$ exhibits a sterically hindered porphyrinic macrocycle that prohibits the generation of H_2 gas,^[8c] the compound is still inert toward N–N coupling and NO reduction.

Although the use of a $\{\text{Fe}(\text{NO})\}^{7/8}$ iron-nitrosyl porphyrin for an N–N coupling reaction is still infeasible, N_2O -evolution activity was established by two-electron reduction of the ligand-constrained non-heme complex $[\text{Fe}_2(\text{BPMP})(\text{OPr})(\text{NO})_2](\text{BPh}_4)_2$ ^[9a] in the absence of an external acid source. Furthermore, the reduction of $\{\text{Co}(\text{NO})\}^8$ $[(\text{Cl})(\text{NO})\text{Co}((\text{Me}^{\text{doen}})\text{Mg}(\text{Me}_3\text{TACN}))(\text{H}_2\text{O}))^+$ in the presence of a proton source, Et_3NHCl , led to N_2O evolution, probably through a bimolecular process,^[9b] which suggests that the reduction of a $\{\text{Co}(\text{NO})\}^8$ cobalt-nitrosyl complex to its corresponding electron-rich $\{\text{Co}(\text{NO})\}^9$ state could potentially produce a reactive species for studying NO-to- N_2O reduction. Herein, we describe the successful reduction of $\{\text{Co}(\text{NO})\}^8$ $[\text{Co}(\text{CTPPMe})(\text{NO})]$ (**1**) to $\{\text{Co}(\text{NO})\}^9$ $[\text{Co}(\text{CTPPMe})(\text{NO})][\text{Co}(\text{Cp}^*)_2]$ (**2**),^[10] which presumably formed a dicobalt dinitrosyl N-confused porphyrin (NCP) intermediate, in which NO-to- N_2O conversion occurred to give $[\text{Co}(\text{CTPPMe})]$, as long as an alcohol (e.g., MeOH or EtOH) or water was introduced to serve as a proton donor through an H-bonding interaction (Scheme 1). To our knowledge, the intermediates for the conversion of axial NO ligands

[*] C.-H. Chuang, Prof. C.-H. Hung
Institute of Chemistry, Academia Sinica
Nankang 11529, Taipei (Taiwan)
E-mail: chhung@gate.sinica.edu.tw

C.-H. Chuang, Prof. W.-F. Liaw
Department of Chemistry, National Tsing Hua University
Hsinchu 30013 (Taiwan)
E-mail: wliaw@mx.nthu.edu.tw

Supporting information and the ORCID identification number(s) for the author(s) of this article can be found under <http://dx.doi.org/10.1002/anie.201512063>.



Scheme 1. Stoichiometric reduction of **1** to **2** ($X^+ = [Co(Cp^*)_2]^+$) and N_2O production through N–N coupling and N–O cleavage as assisted by H-bonding interactions. $Cp^* = 1,2,3,4,5$ -pentamethylcyclopentadienyl.

directly into N_2O on the metalloporphyrinoids have never been identified.

The cobalt–nitrosyl complex $[Co(CTPPMe)(NO)]$ (**1**) was produced from the reaction of $[Co(HCTPP)]^{[11]}$ and excess CH_3I in CH_2Cl_2 , followed by nitrosylation in a THF/MeOH mixed-solvent system under anaerobic conditions in the presence of NaOMe as a base and NO gas (1 %) as the NO source.^[12] The structure of complex **1** was corroborated by single-crystal X-ray structure determination (Figure 1 a), and the complex was characterized by spectroscopic methods. The key structural parameters of **1** include a bent Co–N–O unit with an angle of $125.62(14)^\circ$ and Co–NO and CoN–O bond

lengths of 1.7886(16) and 1.187(2) Å, respectively. The severely bent angle of Co–N–O in **1** is consistent with the structural characteristics of the $\{Co(NO)\}^8$ cobalt–nitrosyl group. The IR spectrum of **1** (KBr) revealed a ν_{NO} vibration at 1620 cm^{-1} ($\nu(^{15}NO) = 1592\text{ cm}^{-1}$; $\Delta\nu_{NO} = 28\text{ cm}^{-1}$); this value is in the regular range for a $\{Co(NO)\}^8$ complex. As compared with other $\{Co(NO)\}^8$ $[Co(porp)(NO)]$ complexes ($\nu_{NO} = 1681, 1677$, and 1710 cm^{-1} for $porp = TPP^{2-}$, OEP^{2-} , and $TPPBr_4NO_2^{2-}$, respectively),^[13] **1** exhibited a lower ν_{NO} value, which suggested that $CTPPMe^{2-}$ is a better electron-donating ligand than the aforementioned porphyrinato macrocycles. Additionally, **1** displayed a low-spin diamagnetic pattern in the 1H NMR spectrum (see Figure S2 in the Supporting Information). The inner methyl group of **1** was located at -4.5 ppm , as confirmed by $[Co(CTPPCD_3)(NO)]$ (**1-CD₃**). The ^{15}N NMR spectrum of $[Co(CTPPMe)(^{15}NO)]$ (**1-¹⁵NO**) exhibited a distinctive signal at 635 ppm (vs. $MeNO_2$; see Figure S4), thus implying a preferential Co^{III} – NO^- electronic state in **1**. Although cobalt–nitrosyl porphyrins can readily provide a $\{M(NO)\}^8$ electronic configuration, as seen in the majority of $\{Co(NO)\}^8$ cobalt–nitrosyl complexes,^[13–15] the reactivity of NO^- in **1** may be stabilized by a kinetically inert low-spin d^6 Co^{3+} center,^[14b] thus making it unreactive without a preceding reduction reaction.

Accordingly, we investigated the reduction of **1** to determine its reactivity, especially in the conversion of axial NO into N_2O . Only a few non-porphyrin-supported $\{Co(NO)\}^9$ cobalt–nitrosyl complexes have been described, and no thorough characterization of a reduced $\{Co(NO)\}^9$ or $\{Co(NO)\}^8$ radical-anion cobalt–nitrosyl porphyrinoid has been reported, possibly as a result of the facile denitrosylation of such compounds upon reduction.^[17a] Furthermore, an electron-rich metal–nitrosyl porphyrin in a reduced state usually requires an electron-deficient porphyrinato ligand for stabilization. For example, $\{Fe(NO)\}^8$ $[Co(Cp)_2][Fe(TFPPBr_8)(NO)]$ was structurally characterized by the use of an extremely electron-deficient porphyrin, $TFPPBr_8^{2-}$, as the supporting ligand.^[16] Consequently, the $CTPPMe^{2-}$ macrocycle was not anticipated to stabilize a reduced complex. However, a reversible redox couple at -0.835 V (vs. SCE; see Figure S5) in a cyclic voltammetry (CV) study and a bathochromic shift of ν_{NO} from the IR spectroelectrochemical (SEC) measurements of **1** imply an unusually stable $\{Co(NO)\}^9$ complex without denitrosylation when **1** receives one reducing equivalent. The reversible redox process at $E_{1/2} = -0.835\text{ V}$ for **1** displayed diffusion-controlled electrochemical behavior, as others have reported for $\{Co(NO)\}^{8/9}$ cobalt–nitrosyl complexes.^[14a, 17b] Upon the electrolysis of **1** in CH_2Cl_2 under -1.2 V (vs. a pseudoreference silver-wire electrode), the IR SEC spectrum showed a ν_{NO} shift from 1616 to 1521 cm^{-1} ($\Delta\nu_{NO} = 95\text{ cm}^{-1}$; Figure 1 b), which was further corroborated by studies with isotope-labeled **1-¹⁵NO** (see Figure S6). Thus far, only one-electron π -ring oxidation of $\{Co(NO)\}^8$ cobalt–nitrosyl tetraaryl porphyrins provided an NO-intact product with $\Delta\nu_{NO} \approx 40\text{ cm}^{-1}$,^[18] all other reduction processes resulted in facile denitrosylation.^[17a] Notably, the one-electron electrochemical reduction of **1** only caused a redshift of the Soret-like band from $\lambda_{max} =$

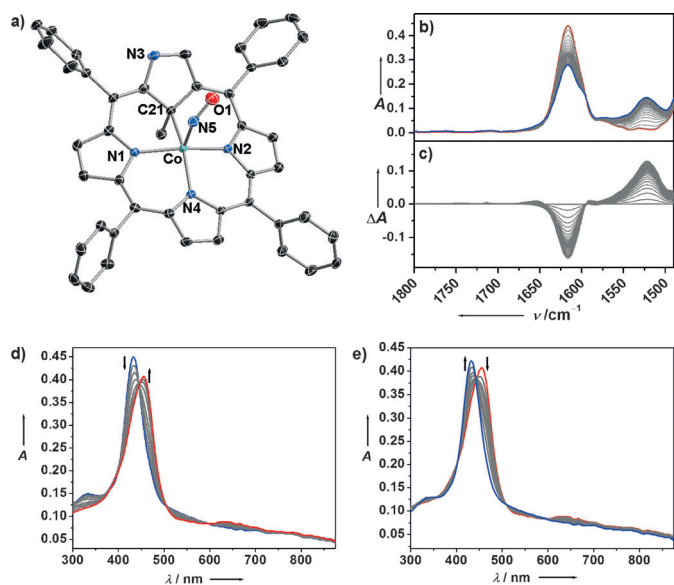


Figure 1. a) ORTEP diagram of **1**. Hydrogen atoms were omitted for clarity. Selected bond lengths [Å] and angles [$^\circ$]: Co–N(5) 1.7886(16), N(5)–O(1) 1.187(2); Co–N(5)–O(1) $125.62(14)$. b) Original and c) subtracted IR SEC spectra of complex **1** under an applied potential (E_{app} vs. Ag wire) of -1.2 V . d, e) UV/Vis SEC spectra of the $1^{0/-}$ ($E_{app} = -1.3\text{ V}$) and $1^{-/0}$ process ($E_{app} = -0.4\text{ V}$), respectively.

432 to 455 nm without significant peak broadening in the UV/Vis SEC spectra (Figure 1). These spectroscopic features from constant potential electrolysis strongly indicated a metal–NO-centered reduction of **1**, in which case it is understandable that reduction of the relatively electron rich CTPPMe²⁻ moiety requires a more negative potential. Significantly, no other stable {Co(NO)}⁹ cobalt–nitrosyl porphyrinoid derived from the electrochemical reduction of the corresponding {Co(NO)}⁸ complex without denitrosylation and with a large $\Delta\nu_{\text{NO}}$ value has been reported to date. Inspired by the CV and IR SEC studies, we attempted to chemically reduce **1** to the {Co(NO)}⁹ complex **2**. The chemical reduction of **1** with [Co(Cp*)₂] (1.2 equiv) in neat THF under anaerobic conditions generated complex **2**, which could be isolated as a crystalline product (89.7%) by saturating the solution of **2** in THF with ether. Similar to the value of 95 cm⁻¹ obtained from IR SEC studies (CH₂Cl₂), the powders of **1** and the chemically reduced compound **2** showed $\Delta\nu_{\text{NO}} = 83 \text{ cm}^{-1}$ (KBr) in the IR spectra.

The quantitative production of **2** with high stability by a chemical reduction reaction in aprotic solvents under anaerobic conditions allowed us to examine its reactivity and the NO reduction intermediates one step at a time. A proton source is proposed to be essential for catalytic NO reduction by NOR. However, the addition of a proton donor (NH₄PF₆) to **2** resulted in H₂ evolution exclusively, accompanied by the regeneration of {Co(NO)}⁸ **1**, in analogy with protonation reactions of {Fe(NO)}⁸ heme–nitrosyl complexes. We then serendipitously observed that the addition of methanol or water to the solution of **2** in THF (protic solvent/THF, 1:1, v/v) is necessary to promote the NO-to-N₂O conversion in association with the disappearance of the characteristic ν_{NO} peak (see Figure S9). N₂O production was confirmed by gas chromatography (GC) of samples taken from the headspace of the reaction vessel (see Figure S10). N₂O production was further corroborated by IR analysis of the headspace gas, which showed characteristic N₂O(g) stretching frequencies at 2236 and 2213 cm⁻¹. These peaks shifted to 2167 and 2144 cm⁻¹ when **1**-¹⁵NO was used as the starting compound, which further confirmed N₂O production from axial NO on the cobalt NCP (see Figure S11). Since the addition of NH₄PF₆ generated H₂(g) exclusively, the pathway of metalloporphyrinoid-irrelevant HNO dimerization to N₂O and H₂O was not the preferred pathway. Although a route to HNO/N₂O generation through proton-coupled nucleophilic attack by aromatic alcohols or ascorbate has been reported, no HNO or N₂O generation with MeOH has been described.^[19]

Besides methanol and water, more sterically bulky alcohols were also applied to the NO-to-N₂O conversion under the same conditions. The replacement of MeOH with EtOH resulted in a much slower N₂O formation rate, which implied direct participation of the alcohol in N₂O formation. Intriguingly, the use of sterically bulky *t*BuOH did not result in N₂O generation (see Figure S10). We therefore concluded that this NO reduction occurred via an intermediate that combined two molecules of **2**. Presumably, a nonplanar NCP core in **2** and sterically bulky *t*BuOH prohibited the dimerization of the two molecules of **2**, although the *pK_a* difference

between the alcohols, and thus the difference in the strength of the H-bonding interactions exerted on the reduced form of **2**, should also be considered. The IR spectrum of **2** in [D₈]THF/[D₄]MeOH (1:1, v/v) strongly supports the presence of an H-bonding interaction between the coordinating NO molecule and methanol, as it shows two distinguishable ν_{NO} humps at 1542 and 1513 cm⁻¹ (Figure 2), which were assigned

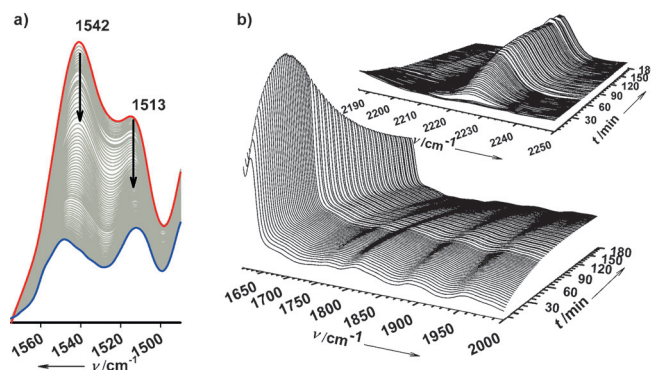


Figure 2. Time-course IR spectra (2–180 min) of **2** dissolved in a) [D₈]THF/[D₄]MeOH (1:1, v/v) and b) THF/methanol (1:1, v/v; inset for N₂O detection).

as **2** and **2**...CD₃OD and which correspond to forms with and without H-bonding interactions between **2** and CD₃OD, respectively. A shift in the ν_{NO} value from 1542 to 1513 cm⁻¹ in the presence of H-bonding interactions with **2** is consistent with the observed back-donation of electron density from a copper–substrate complex to a π^*_{NO} orbital polarized by a H-bonding interaction.^[7] In bioengineered non-heme/heme NOR, the O_{NO} atom of heme–NO electrostatically interacts with a distal metal ion, such as Zn²⁺ or Fe²⁺, in the non-heme pocket, which also decreases the ν_{NO} value up to 50 cm⁻¹.^[20] As DFT calculations on heme–copper oxidoreductase showed that the NO reduction proceeds through an N–N coupling phase facilitated by the protonation of heme–NO to form an HN₂O₂⁻ intermediate, we postulated that treatment with CD₃OD induced the formation of **2**...CD₃OD (shifted to $\nu_{\text{NO}} = 1513 \text{ cm}^{-1}$) through H bonding. It is this polarization that stimulates the interaction between **2** and **2**...CD₃OD and allows N–N coupling to proceed and form a plausible [N₂O₂]-bridged intermediate.

To obtain more data to support the formation of the [N₂O₂]-containing intermediate and to monitor the spectroscopic changes in the whole reaction process for **2** and MeOH, we collected time-resolved IR measurements. When **2** was dissolved in THF/MeOH (1:1, v/v) a new IR peak at 1622 cm⁻¹ appeared immediately and continuously increased during the initial 30 min, after which it decreased (Figure 2b). The use of **2**-¹⁵NO^[10] shifted this peak from 1622 to 1577 cm⁻¹ ($\Delta\nu = 45 \text{ cm}^{-1}$; see Figure S13). This isotope-sensitive peak at 1622 cm⁻¹ is close to the value of $\nu_{\text{NO}} \approx 1605 \text{ cm}^{-1}$ observed for bridging neutral [N₂O₂] coordination in diruthenium complexes that produce N₂O by protonation-induced electron transfer from the diruthenium core to the [N₂O₂] unit.^[4a,b] Furthermore, the concomitant decrease in the bands at 1542

and 1513 cm^{-1} in $[\text{D}_8]\text{THF}/[\text{D}_4]\text{MeOH}$ (Figure 2a), which signifies the consumption of **2** and **2**· CD_3OD , and the increase in the peak at 2224 cm^{-1} in THF/MeOH (2155 cm^{-1} when **2**- ^{15}NO was used; see Figure S13) from the accumulation of N_2O occur concurrently with the intensity change at 1622 cm^{-1} . Thus, we infer that the peak with increasing intensity at 1622 cm^{-1} in THF/MeOH was due to the $\nu(\text{NO})$ vibration of a $[\text{N}_2\text{O}_2]$ intermediate, that is, $[\{\text{Co}(\text{CTPPCD}_3)_2(\mu\text{-N}_2\text{O}_2)(\text{CH}_3\text{OH})\}]^{2-}$, after N–N coupling of **2** and **2**· CH_3OH . The decrease in intensity after a maximum had been reached at 30 min was caused by subsequent N–O fission for N_2O formation. The continuous increase in the intensity of the peak at 2224 cm^{-1} strongly confirmed the formation of N_2O .

Significantly, ESI(–) mass spectrometry (30°C) with MeOH and **2**· $\text{CD}_3^{[10]}$ in THF indicated two sets of m/z patterns corresponding to $[\{\text{Co}(\text{CTPPCD}_3)_2(\text{N}_2\text{O}_2)\}]^-$ (m/z 1437.4) and $[\{\text{Co}(\text{CTPPCD}_3)_2(\text{N}_2\text{O}_2)(\text{OMe})\}]^-$ (m/z 1468.4; Figure 3; see also Figure S14). The observation

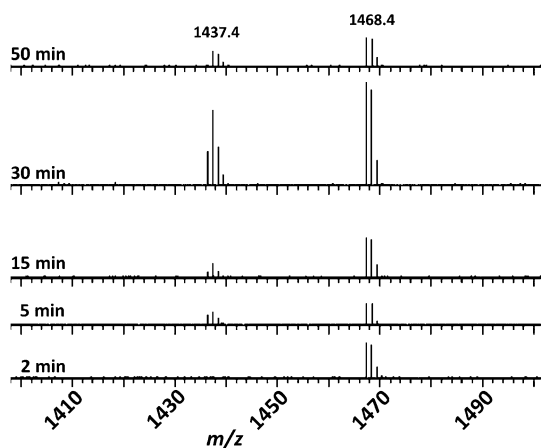


Figure 3. ESI(–) MS spectra (at 30°C ; neat MeOH as the mobile phase) showing signal-intensity changes for the ions m/z 1437.4 and 1468.4 in the reaction of **2**· CD_3 and MeOH from 2 to 50 min.

that the ESI(–) mass signals of these two dimeric fragments exhibited maximum intensity after the reaction had proceeded for approximately 30 min is consistent with the result that the intensity of the peak at 1622 cm^{-1} in the IR spectrum reaches its plateau at 30 min. Although the charge discrepancy between the observed m/z signal and the proposed intermediate cannot be directly correlated with the dianionic intermediate $[\{\text{Co}(\text{CTPPCD}_3)_2(\mu\text{-N}_2\text{O}_2)(\text{MeOH})\}]^{2-}$, the two monoanionic dimers detected in the ESI(–) mass spectrum can be explained by considering them to be the result of oxidation of the authentic intermediate by the ionized proton from MeOH, because the highly reduced intermediates are readily oxidized by protons to form $\text{H}_2(\text{g})$ during electrospray ionization. The use of the $\{\text{Co}(\text{NO})\}^8$ complex **1**· CD_3 for the same measurements in the presence of MeOH produced no corresponding dimeric m/z peak. This observation further signified that an $[\text{N}_2\text{O}_2]$ -containing dimeric cobalt–NCP complex with MeOH polarization is a plausible intermediate. The NO-to- N_2O conversion through a bridging hyponitrite in

combination with a hydrogen-bonded MeOH molecule will generate OH^- through a concerted process involving proton transfer and N–O bond cleavage.

The final denitrosylated complex $[\text{Co}(\text{CTPPCD}_3)]$, which is available for a second reaction cycle, was detected as $[\{\text{Co}(\text{CTPPCD}_3)(\text{OMe})\}]^-$ with m/z 719.2 in the mass spectrum (m/z 716.2 when **2** was used; see Figure S14e). The detection of $[\{\text{Co}(\text{CTPPCD}_3)(\text{OMe})\}]^-$ may also indicate the generation of methoxide (OMe^-) through the deprotonation of MeOH during the NO-to- N_2O conversion. Examination of the $\text{p}K_a$ values of ROH ($\text{R} = \text{H}, \text{Me}, \text{Et}, \text{and } t\text{Bu}$) indicated that $t\text{BuOH}$ is a less effective proton donor than the others and is thus inadequate for promoting N–O bond cleavage and N_2O release. Our results are consistent with the observation that a poor H-bond donor exerts a weaker effect on the NO molecule attached to a Cu(110) substrate.^[7] Finally, after N_2O evolution, the introduction of NO gas into the THF/MeOH solution led to the recovery of **1** (Scheme 1c; see also Figure S9), which was purified and dried for the next N_2O -generation cycle. As many as five reaction cycles were carried out without a significant drop in N_2O production.

In conclusion, we have successfully reduced $\{\text{Co}(\text{NO})\}^8$ **1** to $\{\text{Co}(\text{NO})\}^9$ **2**. Complex **2** is the first $\{\text{Co}(\text{NO})\}^9$ cobalt–nitrosyl porphyrinoid that is stable and has been isolated. The system offers an unprecedented chance to examine the reductive coupling of a $\{\text{Co}(\text{NO})\}^9$ species for N_2O formation. We have provided evidence that a protic solvent acts as an H-bonding donor to drive N–N bond formation and N–O bond cleavage during the NO-to- N_2O conversion. This finding leads us to conclude that the final step of N_2O evolution in NOR may involve concerted N–O cleavage and protonation of the O^{2-} fragment, as induced by buried distal water molecules through H-bonding interactions with the O_{NO} terminus of heme–NO. Furthermore, we propose that the role of distal water in native NOR is not only to shuttle protons but also to trigger N–N bond formation through H-bonding interactions.

Keywords: bioinorganic chemistry · cobalt · N-confused porphyrins · nitric oxide reduction · spectroelectrochemistry

How to cite: *Angew. Chem. Int. Ed.* **2016**, *55*, 5190–5194
Angew. Chem. **2016**, *128*, 5276–5280

- [1] a) I. M. Wasser, S. de Vries, P. Moënné-Loccoz, I. Schroder, K. D. Karlin, *Chem. Rev.* **2002**, *102*, 1201–1234; b) T. Hino, Y. Matsumoto, S. Nagano, H. Sugimoto, Y. Fukumori, T. Murata, S. Iwata, Y. Shiro, *Science* **2010**, *330*, 1666–1670.
- [2] a) N. Yeung, Y. W. Lin, Y. G. Gao, X. Zhao, B. S. Russell, L. Lei, K. D. Miner, H. Robinson, Y. Lu, *Nature* **2009**, *462*, 1079–1082; b) Y. Lu, N. Yeung, N. Sieracki, N. M. Marshall, *Nature* **2009**, *460*, 855–862; c) Y. W. Lin, N. Yeung, Y. G. Gao, K. D. Miner, S. Tian, H. Robinson, Y. Lu, *Proc. Natl. Acad. Sci. USA* **2010**, *107*, 8581–8586; d) Y.-W. Lin, N. Yeung, Y.-G. Gao, K. D. Miner, L. Lei, H. Robinson, Y. Lu, *J. Am. Chem. Soc.* **2010**, *132*, 9970–9972; e) H. Matsumura, T. Hayashi, S. Chakraborty, Y. Lu, P. Moënné-Loccoz, *J. Am. Chem. Soc.* **2014**, *136*, 2420–2431.
- [3] a) J. P. Collman, Y. Yang, A. Dey, R. A. Decréau, S. Ghosh, T. Ohta, E. I. Solomon, *Proc. Natl. Acad. Sci. USA* **2008**, *105*, 15660–15665; b) J. P. Collman, A. Dey, Y. Yang, R. A. Decréau,

- T. Ohta, E. I. Solomon, *J. Am. Chem. Soc.* **2008**, *130*, 16498–16499; c) J. Wang, M. P. Schopfer, A. A. Sarjeant, K. D. Karlin, *J. Am. Chem. Soc.* **2009**, *131*, 450–451.
- [4] a) Y. Arikawa, T. Asayama, Y. Moriguchi, S. Agari, M. Onishi, *J. Am. Chem. Soc.* **2007**, *129*, 14160–14161; b) T. Suzuki, H. Tanaka, Y. Shiota, P. K. Sajith, Y. Arikawa, K. Yoshizawa, *Inorg. Chem.* **2015**, *54*, 7181–7191; c) N. Xu, A. L. Campbell, D. R. Powell, J. Khandogin, G. B. Richter-Addo, *J. Am. Chem. Soc.* **2009**, *131*, 2460–2461; d) A. M. Wright, G. Wu, T. W. Hayton, *J. Am. Chem. Soc.* **2012**, *134*, 9930–9933.
- [5] T. C. Berto, N. Xu, S. R. Lee, A. J. McNeil, E. E. Alp, J. Zhao, G. B. Richter-Addo, N. Lehnert, *Inorg. Chem.* **2014**, *53*, 6398–6414.
- [6] a) T. Ohta, T. Kitagawa, C. Varotsis, *Inorg. Chem.* **2006**, *45*, 3187–3190; b) C. Varotsis, T. Ohta, T. Kitagawa, T. Soulimane, E. Pinakoulaki, *Angew. Chem. Int. Ed.* **2007**, *46*, 2210–2214; *Angew. Chem.* **2007**, *119*, 2260–2264.
- [7] A. Shiotari, S. Hatta, H. Okuyama, T. Aruga, *Chem. Sci.* **2014**, *5*, 922–926.
- [8] a) I. K. Choi, Y. Liu, D. Feng, K. J. Paeng, M. D. Ryan, *Inorg. Chem.* **1991**, *30*, 1832–1839; b) J. Pellegrino, S. E. Bari, D. E. Bikiel, F. Doctorovich, *J. Am. Chem. Soc.* **2010**, *132*, 989–995; c) L. E. Goodrich, S. Roy, E. E. Alp, J. Zhao, M. Y. Hu, N. Lehnert, *Inorg. Chem.* **2013**, *52*, 7766–7780.
- [9] a) S. Zheng, T. C. Berto, E. W. Dahl, M. B. Hoffman, A. L. Speelman, N. Lehnert, *J. Am. Chem. Soc.* **2013**, *135*, 4902–4905; b) C. Uyeda, J. C. Peters, *J. Am. Chem. Soc.* **2013**, *135*, 12023–12031.
- [10] The italic symbols before and after CTPP indicate the substituents on the peripheral nitrogen atom and inner-core carbon atom, respectively; **2-¹⁵NO**: [Co(CTPP*Me*)(¹⁵NO)][Co(Cp*)₂]; **2-CD₃**: [Co(CTPP*CD₃*)(NO)][Co(Cp*)₂].
- [11] C.-H. Hung, C.-H. Peng, Y.-L. Shen, S.-L. Wang, C.-H. Chuang, H. M. Lee, *Eur. J. Inorg. Chem.* **2008**, 1196–1199.
- [12] W.-M. Ching, C.-H. Hung, *Chem. Commun.* **2012**, *48*, 4989–4991.
- [13] a) L. M. Grande, B. C. Noll, A. G. Oliver, W. R. Scheidt, *Inorg. Chem.* **2010**, *49*, 6552–6557; b) M. K. Ellison, W. R. Scheidt, *Inorg. Chem.* **1998**, *37*, 382–383; c) K. M. Kadish, Z. Ou, X. Tan, T. Boschi, D. Monti, V. Fares, P. Tagliatesta, *J. Chem. Soc. Dalton Trans.* **1999**, 1595–1602.
- [14] a) A. K. Patra, K. S. Dube, B. C. Sanders, G. C. Papaefthymiou, J. Conradie, A. Ghosh, T. C. Harrop, *Chem. Sci.* **2012**, *3*, 364–369; b) M. A. Rhine, A. V. Rodrigues, R. J. B. Urbauer, J. L. Urbauer, T. L. Stemmler, T. C. Harrop, *J. Am. Chem. Soc.* **2014**, *136*, 12560–12563; c) P. Kumar, Y.-M. Lee, Y. J. Park, M. A. Siegler, K. D. Karlin, W. Nam, *J. Am. Chem. Soc.* **2015**, *137*, 4284–4287.
- [15] a) M. Di Vaira, C. A. Ghilardi, L. Sacconi, *Inorg. Chem.* **1976**, *15*, 1555–1561; b) S. Thyagarajan, C. D. Incarvito, A. L. Rheingold, K. H. Theopold, *Inorg. Chim. Acta* **2003**, *345*, 333–339; c) N. C. Tomson, M. R. Crimmin, T. Petrenko, L. E. Rosebrugh, S. Sproules, W. C. Boyd, R. G. Bergman, S. DeBeer, F. D. Toste, K. Wieghardt, *J. Am. Chem. Soc.* **2011**, *133*, 18785–18801.
- [16] B. Hu, J. Li, *Angew. Chem. Int. Ed.* **2015**, *54*, 10579–10582; *Angew. Chem.* **2015**, *127*, 10725–10728.
- [17] a) K. M. Kadish, X. H. Mu, X. Q. Lin, *Inorg. Chem.* **1988**, *27*, 1489–1492; b) C.-Y. Chiang, J. Lee, C. Dalrymple, M. C. Sarahan, J. H. Reibenspies, M. Y. Darensbourg, *Inorg. Chem.* **2005**, *44*, 9007–9016.
- [18] A. D. Kini, J. Washington, C. P. Kubiak, B. H. Morimoto, *Inorg. Chem.* **1996**, *35*, 6904–6906.
- [19] S. A. Suarez, N. I. Neuman, M. Muñoz, L. Álvarez, D. E. Bikiel, C. D. Brondino, I. Ivanović-Burmazović, J. L. Miljkovic, M. R. Filipovic, M. A. Martí, F. Doctorovich, *J. Am. Chem. Soc.* **2015**, *137*, 4720–4727.
- [20] T. Hayashi, K. D. Miner, N. Yeung, Y. W. Lin, Y. Lu, P. Moënne-Loccoz, *Biochemistry* **2011**, *50*, 5939–5947.

Received: December 31, 2015

Revised: February 8, 2016

Published online: March 22, 2016